CHAPTER I. INTRODUCTION

I.1-- THE PRINICPLES OF TIME-OF-FLIGHT MASS SPECTROMETRY

Time-of-flight mass spectrometry (TOF-MS), a *separation-in-time* technique, is unlike magnetic sector and quadrupole mass analyzers in which ions are *spatially separated*. TOF-MS begins with gas-phase ion formation and then ion acceleration through an electric field into a field-free drift region. The acceleration voltage, giving all ions the same kinetic energy, propels the ions at different velocities based on their specific mass-to-charge (normally singly charged species are produced) ratios. Subsequently, the ions are allowed to drift under no external field and separate as a function of their individual velocities (masses). Smaller ions will simply move faster than larger ions for mass separation. Following ion detection, "peaks" representing isomass ion-packets comprise the mass spectrum, and the time needed to travel the length of the drift region (the "time-of-flight") can be related to the mass of the ion.

I.2-- ADVANTAGES/DISADVANTAGES OF TOF-MS

Time-of-flight instruments have numerous advantages over "traditional" quadrupole and magnetic sector mass analyzers. The virtually unlimited upper-mass limit of TOF-MS has made it popular and nearly exclusive for high-mass applications, as molecules of 1,000,000 amu and greater have been analyzed[1]. Since a complete mass spectrum is generated in only microseconds, the "instantaneous" data acquisition allows signal-averaging to increase the signal-to-noise ratio in short analysis times. In contrast to magnetic sector and quadrupole instruments, the higher sensitivity afforded in the "all at once" TOF instrument can be substantial; there is no need to scan through radio frequencies or voltages to sequentially select certain ions while discarding others. Furthermore, sample preparation for TOF-MS introduction can be minimal, especially with solids analysis. Direct sampling of solids with little "clean up" is common and minimizes contamination to maintain sample integrity. Also for solid samples, spatial resolution on a micrometer scale is possible with laser-ionization time-of-flight mass

[1] K. Bush. *Spectroscopy*. **12** (1997) 22.

spectrometry (LI-TOF-MS) techniques. Another advantage of TOF-MS is the simplicity and ease of construction of time-of-flight systems, with few moving parts and a straightforward design.

For years, the main limitation with TOF instruments has been the poor resolution when compared to other mass analyzers. Even modern linear systems generally have resolution capabilities of no better than 300-400[2]. Although improvements have been made, the simplicity of the linear time-of-flight system is often compromised. Another drawback is the difficulties in interfacing TOF-MS as a mass analyzer with a continuous ion source. Continuous sources, such as chromatographic effluents, place high demands on the pumping system and do not match well with the ion bursts required for the time-of-flight analysis.

I.3-- HISTORY OF TOF-MS

After time-of-flight as a mass separation technique was originally proposed in 1946[3] the first time-of-flight mass spectrometer was constructed by Cameron and Eggers in 1948[4]. Although resolution limitations plagued the early instruments, incorporating pulsed electron impact sources provided a significant achievement in the early 1950's. The most outstanding contribution to resolution improvements arose from the fundamental TOF-MS publication by Wiley and McLaren in 1955[5], in which they systematically treated resolution-limitation problems. Amazingly relevant even to the most modern TOF instruments, Wiley and McLaren's benchmark paper analyzed both instrumentally and mathematically the major causes of mass resolution problems of the time-of-flight technique. Practical application of their ideas, however, still left mass resolution in the low hundreds. The first commercial TOF device was produced in 1957, but interest in TOF-MS waned in the 1960's due to the popularity of magnetic sector and quadrupole instruments. The sensitivity, resolution, and interfacing capabilities of these

[2] R. Cotter. Chap. 1, in R. Cotter, Ed. *Time-of-Flight Mass Spectrometry*. Proceedings of the 204th National Meeting of the ACS and Pittsburgh Conference on Analytical Instrumentation. American Chemical Society, Washington, D.C., 1994.

[3] W.I. Stephens. *Phys. Rev*. **69** (1946) 691.

[4] A.E. Cameron, D.F. Eggers. *Rev. Sci. Instrum*. **19** (1948) 605.

[5] W.C. Wiley, I.H. McLaren. *Rev. Sci. Instrum*. **26** (1955) 1150.

mass analyzers left TOF-MS in a stage of slow development. Limitations in electronics and detection methods hindered progress as well, as slow, non-recording oscilloscopes often could not handle the microsecond time frame of the TOF experiment and required laborious spectral accumulation. Applications of TOF-MS during this time centered on research studies of gas-phase reactions, such as flash pyrolysis and photolysis products, gas decompositions, and reaction rates.

With interest lacking, TOF-MS might have faded completely had lasers not been developed. Pulsed lasers provided ideal ion sources for the TOF instrument, and "laser mass spectrometers" probed surface compositions in the mid-1960's. Although the first European TOF-MS Symposium was held in 1967, only about 300 TOF-MS instruments were currently in use worldwide[2]. Concurrent improvements in laser technology kept some interest in TOF systems, but the "traditional" magnetic sector and quadrupole instruments dominated mass spectrometry through the 1970's.

The instrumental innovation of the "reflectron" by Mamyrin[6] in the early 1970's to correct for the large initial kinetic energy distributions imparted to the analyte ions during laser ionization was a monumental breakthrough for improved mass resolution. The reflectron opened new avenues for laser ionization, but the "traditional" mass analyzers still relegated TOF devices for specific purposes such as solid surface analyses and depth profiling. In the mid-1980's, some resurgence in the TOF technique accompanied the development of new desorption and ionization sources such as plasma or laser desorption followed by secondary laser ionization.

Leading to a renaissance in TOF-MS in the 1990's, matrix-assisted-laser-desorption/ionization (MALDI-TOF) techniques introduced by Hillenkamp[7] in 1987 enable the analysis of high-mass species otherwise incapable of mass-spectrometric detection. Uniquely able to handle the high masses of large biomolecules (1000's of amu), TOF-MS has been crucial for the analysis of proteins, peptides, and other biologically significant species. Applications have expanded to the sequencing of DNA, and the MALDI-TOF technique has even been extended to polymer analysis. The near future should see continued MALDI-TOF applications and high-mass analyses.

---

[6] B.A. Mamyrin, D.V. Schmikk, V.A. Zagulin. *Soviet Phys. JEPT.* **37** (1973) 45.

[7] M. Karas, D. Bachman, U. Bahr, F. Hillenkamp. *Int. J. Mass Spectrom. Ion Processes.* **78** (1987) 53.

I.4-- THE TIME-OF-FLIGHT MASS SPECTROMETER AND RELATED INSTRUMENTATION

I.4.1-- Basic System

Time-of-flight mass spectrometers can be simple devices or customized for novel, complex analyses. A basic, single-stage linear design requires only a source of ions, an extraction/acceleration voltage plate, a field-free drift tube, an ion detector, and a vacuum system (see Figure I.1(a)). Typical acceleration voltages vary, but generally range from 1 kV to 30 kV. Modifications for enhanced performance, such as a triple electrode ("dual-stage") ionization chamber increases experimental optimization. In contrast to the two electrode ("single-stage")(Figure I.1(a)) design, the dual-stage configuration separates the ionization/acceleration region into (i) an extraction region with a dedicated extraction (repelling) plate and (ii) an acceleration region with an acceleration (attracting) plate (Figure I.1(b)).

I.4.2-- Reflectron devices

The reflectron, introduced by B.A. Mamyrin in 1973[6] to enhance resolution, has proven perhaps the most significant instrumental development in TOF systems. The reflectron is an ion mirror consisting of a series of grids/lenses in either a single-stage (two-electrode) or dual-stage (three-electrode) design (see Figures I.3 and I.4). In most cases, there is an offsetting angle of a few degrees from the primary drift tube to the second field-free drift tube after the reflecting device. To achieve maximum transmission and minimal ion packet divergence[8], the ion detector at the end of the second flight tube is aligned parallel to the reflector grids. Although field distortions and ion scattering at the reflectron are possible, this innovation has been crucial for resolution improvements and the resurgence of TOF-MS.

[8] B. A. Mamyrin. *Int. J. Mass Spectrom. Ion Processes.* **131** (1994) 1.

TOF INSTRUMENT CONFIGURATIONS: (a) LINEAR and (b) REFLECTRON

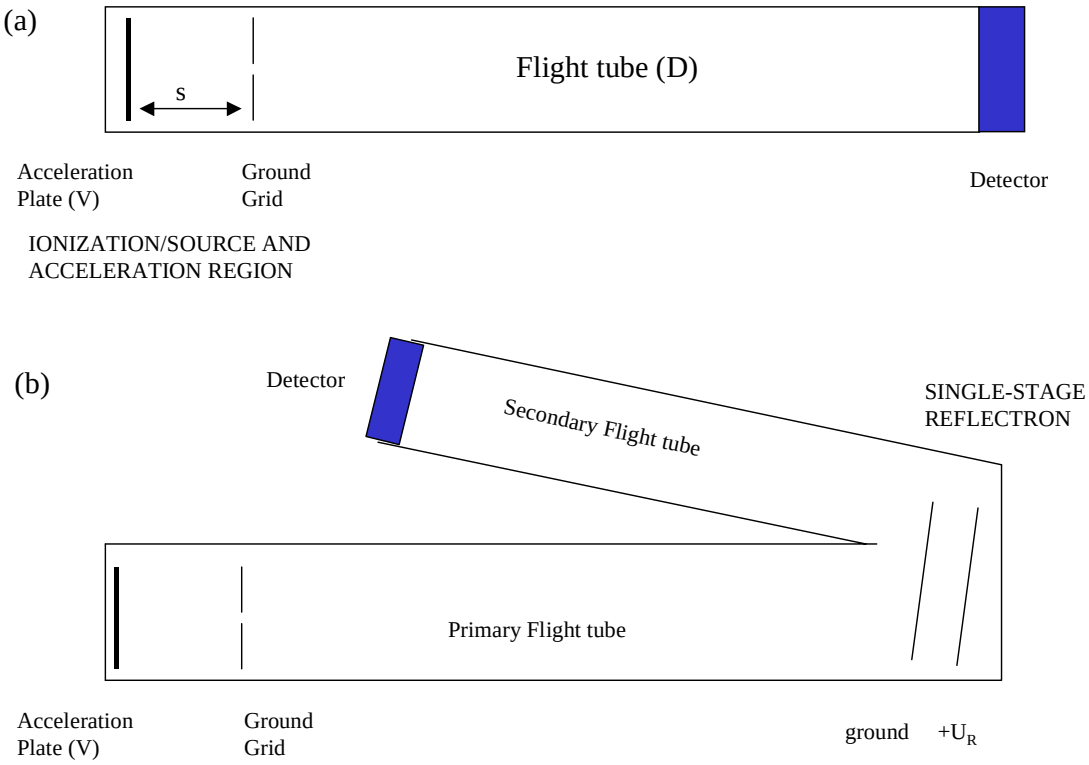

Figure I. 1 (a) Linear geometric configuration Time-of-Flight mass spectrometer and (b) Single-stage reflectron Time-of-Flight mass spectrometer.

I.4.3-- Ion detectors

Most TOF-MS systems incorporate an electron multiplier for ion detection. Dynode "cups" and Chevron or multichannel plates are common designs. Upon impact by an ion of sufficient energy, an electron burst is produced and subsequently amplified by several dynodes. The electron current output from the detector is then interfaced to an oscilloscope or other waveform-recording device.

I.4.4-- Waveform display

Display electronics have progressed considerably since the early days of TOF-MS and are a key instrumental development for TOF systems. Early methods employed a continuous dynode electron multiplier linked to a non-digitizing oscilloscope. To display a complete time spectrum, laborious "slice" accumulation techniques were necessary. This method recorded the time-of-flight spectrum on the oscilloscope in separate 10-40 ns intervals for repeated ion pulses. Incrementing in an identical 10-40 ns step and adding the results sequentially (e.g. 0-10 ns, 10-20 ns, etc.) for ~1000 ion pulses allowed a complete time-of-flight spectrum of perhaps 100 μs to be recorded. Hard copies were then obtained by photographing the oscilloscope screen.

Analog-to-digital converters (ADC's) replaced such "slice" methods, and rapid ADC's have developed into the fast oscilloscopes employed today. Digitization with these waveform recorders allows complete spectral acquisition for each ion pulse and signal-averaging capabilities. Speeds of modern oscilloscopes have reached 1 Gigasamples/second at bandwidths of 500 Megahertz or greater.

I.4.5-- TOF-MS Data

Typical waveforms from the oscilloscope display the intensity (-Voltage) as a function of the time-of-flight (seconds). Signal "peaks" arise from isomass ion packets, and the time-of-flight is defined at the peak centroid. The peak width (Δt_{FWHM}) reveals the sharpness, or resolution, of the data. After mass calibration to convert the time-of-flight into a mass-to-charge (M/Z) value, a mass spectrum of ion intensity versus mass, similar to that from other mass analyzers, is obtained.

I.5-- NEUTRAL SOURCES AND IONIZATION METHODS

Due to the burst of ions necessary for the TOF experiment, matching the source of neutral sample with the ionization technique is crucial. Neutral species may be generated by a number of different techniques. Gaseous neutral samples from an effusive nozzle source or supersonic beams are efficiently laser-ionized[9,10], and pulsed supersonic molecular beams provide a good source for subsequent laser ionization[11]. Interfaces with continuous sources preceeding ionization by Fast-Atom-Bombardment (FAB), Electrospray Ionization (ESI), and Atmospheric Pressure Ionization (API) are possible, but pumping requirements limit their flexibility. These instrumental difficulties limit TOF-MS as a mass detector for gas or liquid chromatography. Sample introduction following capillary electrophoresis (CE) has been more successful because the low solvent volumes of CE ease the TOF-MS pumping requirements. Further possibilities include inductively coupled plasma (ICP) ion generation for solution samples.

Desorption techniques, where the analyte is removed from a surface as a neutral species, are popular with solid samples. Common examples include sputtering with an inert atom beam, thermal activation, and laser methods. Although not a true "desorption" technique, plasma desorption, where fission fragments from a radioactive source (e.g. ^{252}Cf) impact the solid sample to release ions, has been used almost exclusively with TOF mass analyzers[12]. Many of the newer desorption methods are laser-based, and both continuous-wave and pulsed lasers have been employed. By carefully controlling the energy density, the identity of the removed species can be varied as higher laser fluences promote fragmentation[13]. Following species production from the surface, secondary ionization is typically performed by laser ionization of the desorption products a few millimeters above the sample surface.

Pulsed ionization methods, commonly lasers, are perhaps the most common ion-producing sources for modern TOF-MS. Before laser instruments, electron impact was

[9] D. Lubman, R. Jordan, *Rev. Sci. Instrum.* **56** (1985) 373.

[10] P. Strupp, A. Alstrin, R. Smilgys, L. Leone. *Applied Optics.* **32** (1993) 842.

[11] U. Boesl, R. Weinkauf, C. Weickhardt, E. Schlag. *Int. J. Mass Spectrom. Ion Processes.* **131** (1994) 87.

[12] R. Cotter. *Anal. Chem.* **64** (1992) 1027A.

[13] T.V. Venkatesan. Chap. 4, in J. Miller, Ed. *Laser Ablation—Principles and Applications.* New York: Springer-Verlag, 1994.

popular in early TOF-MS studies because of the ease of pulsing these sources[14]. Continuous electron impact methods have developed considerably as trapping techniques[15,16,17] such as ion traps can accumulate and subsequently release the stored ions. Ion packets from continuous sources can also be produced and selected through pulsed extraction fields or ion gating/retarding methods.

I.5.1-- Laser ionization

Laser ionization, desorption, and ablation are complex processes. For this discussion, focus will be placed on the ablation technique for solids analysis as used in our LI-TOF-MS. A brief overview of other methods will be mentioned, as these issues have been treated thoroughly in other sources[18,19,20,21]. Although ablation, ionization, and desorption are quite similar, our current context will separate the three into distinct processes. Laser "ablation", defined as the direct removal of ions from the sample surface, differs slightly from the general term of laser ionization. "Ionization" typically refers to the creation of ions from any neutral species. "Desorption" is considered a removal of neutral species by laser radiation.

I.5.1.1-- Advantages of laser-ionization TOF-MS

Laser ionization mates well with TOF instruments, and Laser Ionization Time-of-Flight Mass Spectrometry (LI-TOF-MS) has developed into a highly sophisticated analytical tool since the 1970's. Primarily, the pulsed nature of many modern lasers makes them ideal for efficiently producing ion bursts compatible with TOF-MS.

---

[14] P.Y. Cheng, H.L. Dai. *Rev. Sci. Instrum.* **64** (1993) 221.

[15] O. Gruner, G. Li, H. Stroh, H. Wollnik. *Int. J. Mass Spectrom. Ion Processes.* **93** (1989) 323.

[16] B. Chien, S. Michael, D. Lubman. *Int. J. Mass Spectrom. Ion Processes.* **131** (1994) 149.

[17] S. Michael, B. Chien, D. Lubman. *Rev. Sci. Instrum.* **63** (1992) 4277.

[18] D. Lubman. *Anal. Chem.* **59** (1987) 31A.

[19] B. M. Tissue. *Appl. Spec. Rev.* **29** (1994) 367.

[20] K.G. Standing, W. Ens. Eds. *Methods and Mechanisms of Producing Ions From Large Molecules*. New York: Plenum Press, 1990.

[21] D. Lubman, Ed. *Lasers and Mass Spectrometry*. New York: Oxford University Press, 1990.

Combining the fast laser repetition rates (up to 10 kHz[22]) with instant TOF mass spectral acquisition, a series of laser shots can be averaged to increase the signal-to-noise ratio (Multiplex advantage)[23] in a minimal amount of time. The efficiency of laser ionization techniques maximizes sensitivity, and only a small sample quantity is required for analysis. Also, the tight laser focus allows for spatial analyses on the order of 1μm[24] and laser-based methods are ideal for spatially characterizing solid samples. Laser ablation is particularly popular for its experimental simplicity, as a solid can be analyzed with minimal sample preparation and instrumental complexity.

I.5.1.2-- Disadvantages of laser-based methods

Two main limitations of laser ionization, low precision and quantitation of the ion yields, have been extensively studied since the inception of LI-TOF-MS. Traditionally, laser ablation has suffered from a lack of reproducibility in the number of ions that are produced with repetitive laser shots. Thus, although the integration of the area under a mass spectral peak should directly reveal the ion yield (Equation I.1), this simple technique is rarely employed for quantitative analysis, and elaborate procedures are required even for semi-quantitative work. Also, non-representative analyses are common due to preferential vaporization and/or ionization of certain species from a heterogeneous sample. Resolution limitations due to the initial kinetic energy distributions among isomass ions caused by the laser ablation process[2] are other drawbacks with LI-TOF-MS. Furthermore, the small sampling volume of the laser beam makes bulk analyses difficult[25].

I.5.1.3-- Customizing laser ionization

The variety of laser ionization methods and neutral sources enables a wide range of analyses. The flexibility of laser ionization methods allows for enhanced selectivity and/or sensitivity when desired. Choices for the wavelength, beam focus, and beam

[22] P. Voumard, Q. Zhan, R. Zenobi. *Rev. Sci. Instrum.* **64** (1993) 2215.

[23] C. Becker. Chap. 4, in D. Lubman, Ed. *Lasers and Mass Spectrometry*. New York: Oxford University Press, 1990.

[24] M. Savina, K. Lykke. *Anal Chem.* **69** (1997) 3741.

[25] C. Chen, M. Payne, G. S. Hurst, S. Kramer, S. Allman, R. Phillips. Chap. 1, in D. Lubman, Ed. *Lasers and Mass Spectrometry*. New York: Oxford University Press, 1990.

energy are some simple ways to customize an analysis. Possible techniques range from non-selective ablation (direct ionization) by bombardment with highly energetic laser pulses to species-selective resonance-enhanced multiphoton ionization (REMPI) where the laser is tuned specifically to a resonance of the chosen analyte. Thus, the method of laser ionization can be tailored to each particular analysis, and high efficiencies are achieved especially with resonance-enhanced techniques[8]. Also, the selectivity of resonance ionization minimizes interferences. Between these two extremes of simplicity and sophistication, selection of the laser energy density enables some control over fragmentation of the analyte. Especially noteworthy are "soft" ionization possibilities to produce molecular ions of fragile molecules. Furthermore, matrix-assisted-laser-desorption/ionization (MALDI) techniques combined with the high-mass capabilities of TOF-MS have exploded in the 1990's in the analysis of biomolecules, as will be discussed in detail in Chapter VI. In addition, the removal of neutral species from the sample surface (desorption) can be decoupled from ionization in a "post ionization" technique as two lasers are used in conjunction to optimize the desorption and ionization steps separately.

I.5.1.4-- Laser-material interactions

Particularly relevant for our data are the interactions between laser radiation and a solid sample. Impediments in the quantitation and precision of LI-TOF-MS revolve around the complex and not well understood laser-material interactions[26]. Factors governing these interactions and the ablation yield may be broken into two categories, (i) material properties and (ii) laser properties. Each of these factors will affect both the removal of material from the surface ("desorption") and the ionization of species that are produced.

Laser-sample interactions are complicated processes. Generally, an intense microplasma plume is generated at the solid sample surface by high-energy laser radiation. This plasma consists of a wide range of products including atoms and atomic ions, molecules and molecular ions, clusters and cluster ions, and molecular fragments

[26] R. Odom. B. Schueler, Chap. 5, in D. Lubman, Ed. *Lasers and Mass Spectrometry*. Oxford University Press, 1990.

and fragment ions[13,27]. Since the ease of desorption governs the relative yield of each of these species, the volatilities, thermal conductivities, and enthalpies of atomization are important material properties. Furthermore, other properties such as the boiling, melting, and sublimation points, as well as the surface morphology dictate the amount of material leaving the surface.

Secondly, the ease of ionization highly affects the identities of each particular species that exists in the microplasma. Absorption coefficients, electron affinities, and ionization potentials are substantial material properties affecting the relative yields of non-ionized-to-ionized species. Of course, most of these properties cannot be linked to either desorption or ionization exclusively, and the interactions are indeed complex.

As a result, fractionation and non-representative yields are common due to both the preferential desorption and ionization of particular species in a given sample composition and chemical environment. Broadly termed "matrix effects", the relative ionization responses generally follow the ionization potentials[28], but this fails to consider the additional fractionation during desorption. Furthermore, because sample morphology affects the ion production, even a homogenous sample may likewise portray inconsistent ion yields.

Laser properties are also integral aspects of the ablation process. The wavelength and intensity of the laser beam are the most obvious features that affect the ion yield. In addition, the laser pulse width and repetition rate impact the heat dissipation (and thus the ease of desorption) of the material. Finally, the output stability of the laser is crucial. Advances in laser technology have aided quantitation and reproducibility, but deviations in the shot-to-shot reproducibility of the laser energy can be up to 10%[29].

I.5.2-- Corrective measures for improved reproducibility and quantitation

Several methods address the quantitation and reproducibility problems of LI-TOF-MS analyses. Operating at high laser fluences which largely exceed the ionization

[27] K. Dittrich, R. Wennrich, Chap. 5, in J. Sneddon, Ed. *Sample Introduction in Atomic Spectroscopy*. New York: Elsevier, 1990.

[28] K. Lykke, D. Parker, P. Wurz, J. Hunt, M. Pellin, D. Gruen, J. Hemminger. *Anal. Chem.* **64** (1992) 2797.

[29] W. Sdorra, K. Niemax. *Spectrochim. Acta.* **45B** (1990) 917.

potentials of all of the species to be analyzed has reduced fractionation[26,30]. Also, fusion techniques of grinding the sample in a binder mix have been employed[30]. Most successful semi-quantitative work, though, generates Relative Sensitivity Factors (RSF's) for each analyte in the sample[26,31]. This somewhat laborious procedure involves preparing and analyzing standards of each particular element in a matrix similar to the sample composition. Based on the responses of each element, RSF values are obtained, and the intensity data from the actual sample scaled accordingly. The accuracy and precision of the RSF approach, therefore, largely depends on how well the standard matrices match the actual sample matrix. A common example involves doping an epoxy resin matrix with the analytes. This method has been used jointly with an internal standard for successful semi-quantitative work on the amount of iron in human tissue.[26].

Although a main advantage of direct, single-laser ablation (desorption and ionization) from the sample surface is its simplicity, the two steps may be decoupled in a "post-ionization" technique. As such, desorption of the neutral species and subsequent post-ionization may be optimized separately for sensitivity and/or selectivity of the species to be detected, and semi-quantitative work is possible with reproducibilities better than 90%[27]. In addition to the increases from separate optimization, the greater stability of the neutral species yield in the desorption process[23] over directly produced ions enhances precision.

Such correction methods as Relative Sensitivity Factors and post-ionization have made strides in the last decade, but, as Odom and Schueler claim, "a rather comprehensive understanding of the pertinent fundamental processes is required before quantitative methods can be developed"[26].

I.5.3-- Number of ions detected

Peak area data obtained after integration experimentally estimates the number of ions detected. The output from most multichannel plate detectors, an electrical current, is directly related to the number of ions that strike the multichannel plate. By knowing the

[30] E. Cromwell, P. Arrowsmith. *Anal. Chem.* **67** (1995) 131.

[31] R. Mansoori, M. Johnston, A. Wexler. *Anal. Chem.* **66** (1994) 3681.

termination resistance and the gain of the detector, the following relation estimates the number of ions contained in a given peak[26]:

$$i_p = \frac{NGq}{\Delta t}$$

Equation I. 1: Number of ions contained in a mass spectral peak.

where G is the gain of the detector, i_p is the peak current, Δt is the peak width, q is the charge of an electron, and N is the number of ions detected. Integration of the area under the peak is therefore $i_p \times \Delta t$.

I.6-- THEORY OF MASS SEPARATION BY TOF-MS

The original, linear mass spectrometers illustrate the fundamental TOF-MS principles and the TOF technique. Considering Figure I.1(a), the concepts and equations related to mass separation can be developed. Ions are first formed in the short source/ionization region, usually with a pulsed ion source, and the time recording process is initiated. The potential applied to the acceleration/extraction plate accelerates the ions out of the source region and into the field-free drift region. As long as the acceleration pulse lasts as long or longer than the time of ionization, all of the ions will be imparted with the same kinetic energy, given by Equation I.2:

$$U = zeV$$

Equation I. 2: Kinetic energy of an ion due to an applied potential.

where U is the kinetic energy of the ion, V is the applied potential, and z and e refer to the charge on the ion an electron, respectively.

The same kinetic energy accelerating the ions, however, translates into a range of velocities based on the mass-to-charge (m/z) ratios of the ions, since the kinetic energy is related to the velocity (v) of the ion through Equation I.3

$$U = \tfrac{1}{2} mv^2$$

Equation I. 3: Velocity-kinetic energy relation.

and rearranging after substituting Equation I.2,

$$v = \sqrt{\frac{2zeV}{m}}$$

Equation I. 4: Ion velocity following the acceleration pulse (V).

It is the inverse relation of mass and velocity as shown in Equation I.4 which underlies the TOF-MS technique. Considering all singly charged species, the smaller ions move faster through the drift tube and separate from the slower-moving large masses. This is the governing principle of *separation-in-time*.

Assuming that most of the ion's flight time (t) is spent in the drift tube (D>>s), the time-of-flight can be determined through

$$t = \frac{D}{v} = D \times \sqrt{\frac{m}{2zeV}}$$

Equation I. 5: Time-of-flight of an ion through the mass spectrometer.

Rearranging this equation provides the conversion of the time-of-flight data into a direct mass-to-charge relation:

$$m/z = 2eV\left(\frac{t}{D}\right)^2$$

Equation I. 6: Conversion of flight time to mass.

If the precise dimension of the drift tube (D) and the applied acceleration potential (V) are known, the m/z ratio and ion identity are determined from the time-of-flight.

Numerous points should be highlighted regarding these general principles. In most cases, the ionization source is pulsed, and the time-of-flight is defined as beginning at the time of ionization (for constant acceleration potential). Alternatively, when a continuous ion source is employed, or in other cases when the acceleration voltage is pulsed, the time-of-flight initiates at the acceleration pulse. In addition, the bias of the acceleration pulse determines the identities of the masses that are analyzed. Again referring to the simple linear configuration of Figure I.1(a) and physical concepts, a positive acceleration voltage will propel only positive ions into the drift region for separation. Similarly, only negative ions can be detected if the bias is reversed. The desired analysis thus determines the instrumental configuration, but the mathematics is similar.

In theory, Equation I.5 implies that infinite mass separation can be achieved if the times-of-flight of the ions are infinitely long. This is possible if the drift length (D) is extremely long, and/or the acceleration voltage (V) is extremely low. However, practical instrumental considerations and compromises eliminate such approaches.

I.7-- MASS CALIBRATION

In a linear TOF-MS instrument, approximate mass-to-charge ratios can be determined directly in an "External Calibration" fashion from Equation I.6 if the exact drift length and acceleration potential are known. Unlike magnetic sector and quadrupole calibrations, though, the direct relation is rarely used. In most cases, calibration for TOF-MS is performed from empirical determination of the times-of-flight of several known masses. Subsequently, a calibration line is drawn, according to

$$m/z = at^2 + b$$

Equation I. 7 : Empirical mass calibration equation.

and the calibration constants a and b are determined through a least-squares linear regression to provide more accurate "Internal Calibration". Any experimental time-of-flight (t) can then be converted to a m/z value to identify the unknown ions. Similar calibration methods apply also with reflectron instruments, although the calibration constants will differ from the values obtained in a linear TOF-MS instrument.

I.8-- RESOLUTION

Broadly defined, resolution is the ability to distinguish two ions of different masses, and is usually scaled to the mass range under consideration, such that

$$R = \frac{m}{\Delta m}$$

Equation I. 8: General resolution definition.

where R is the resolution, Δm is the difference in mass of the species, and m is the average mass of the two ions.

Referring specifically to TOF-MS and assuming a single charge on the ion, the resolution equation can be rearranged to yield

$$R = \frac{t}{2\Delta t_{FWHM}}$$

Equation I. 9: Resolution equation for TOF-MS.

where the Full Width at the Half-Maximum (FWHM) of the peak, Δt_{FWHM}, has replaced the masses of the two separate ions. This enables resolution estimates for any given mass based solely on the time-of-flight and peak width.

Thus, it is clear that an increased time-of-flight, t, (long drift length and/or low acceleration potential) or narrowed peak width (Δt_{FWHM}) maximizes resolution. Ideally, this could be done simultaneously, but system parameters usually affect t and Δt_{FWHM} in opposite manners, and all peak-widening factors must be considered to select the parameters for TOF-MS operation.

I.8.1-- Limitations to resolution

Peak broadening (resolution limiting) factors are plentiful in TOF-MS. The two major resolution-hindering factors can be broadly grouped as (i) spatial distributions (σ_s) and (ii) initial energy (velocity) distributions (σ_v) of isomass ions in the source region[8]. Temporal distributions of ion formation times (σt_0) comprise a third general peak-broadening category. In essence, all broadening (Δt) sources can be categorized under one of these three headings so that:

$$f(\Delta t) \approx f(spatial), f(energetic), f(temporal)$$

Equation I. 10: Time-of-flight distribution factors.

The contribution of each factor is essentially Gaussian in nature[32], and the total variance (σ_t) in the time-of-flight of same-mass ions in the ion packet can be approximated statistically as

$$\sigma_t^{\,2} = (\partial t / \partial s_0)^2 \sigma_s^{\,2} + (\partial t / \partial v_0)^2 \sigma_v^{\,2} + \sigma_{t_0}^{\,2}$$

Equation I. 11: Total variance in the time-of-flight of isomass ions due to initial spatial, velocity, and temporal distributions.

[32] M. Guillhaus. *J. Mass Spectrom.* **30** (1995) 1519.

I.8.2-- Initial spatial distribution and the primary space focus

A significant spatial distribution, that is, the position of an ion at the moment of the extraction pulse, contributes highly to peak broadening. Such effects have been extensively noted and treated beginning with the fundamental Wiley-McLaren paper in 1955[5] and continuing to the present. A pictorial representation highlights the problem, as Figures I.2(a) and I.2(b) show three isomass ions at different locations at the moment of the extraction pulse. The variations of ion position are due to factors such as (i) the finite size of the laser focus (assuming laser ionization), (ii) the distribution of ion positions following the laser ablation/desorption process, (iii) space-charge collisions, and (iv) effusion of ions or neutrals from a spray needle or nozzle.

Considering the simple single-stage extraction/acceleration ion region depicted in Figure I.2(a), a difference in the flight length and time of the three ions is obvious. Taking ion 2 as the mean initial position, s_0, and assuming that ions 1 and 3 are the same distance from s_0, ion 1 travels a longer path, $s_0 + \Delta s$, while ion 3 travel a shorter distance, $s_0 - \Delta s$. However, a second factor affects the time-of-flight of these isomass ions, since they will "feel" different proportions of the extraction field voltage due to their relative proximities to the acceleration plate. With ion 1 experiencing a higher acceleration, its velocity increase will allow it to catch up to the ions of shorter flight paths, since the energy increase/decrease is position-dependent as well, according to Equation I.12

$$\Delta U = (s_0 \pm \Delta s) E_s q$$

Equation I. 12: Change in acceleration energy as a function of initial ion position.

where ΔU is the change in energy from the mean formed at s_0, and E_s is the electric field strength (Volts/s).

The point (plane) of "catch-up", where ΔU vanishes[33], corrects the initial spatial distributions as isomass ions pass this first-order, *primary space-focus* at the same time, as is displayed conceptually in Figures I.2(a) and I.2(b). In the simple one-stage extraction/acceleration system shown in Figure I.2(a), the space-focus point is strictly

[33] U. Boesl, R. Weinkauf, E. Schlag. *Int. J. Mass Spectrom. Ion Processes.* **112** (1992) 121.

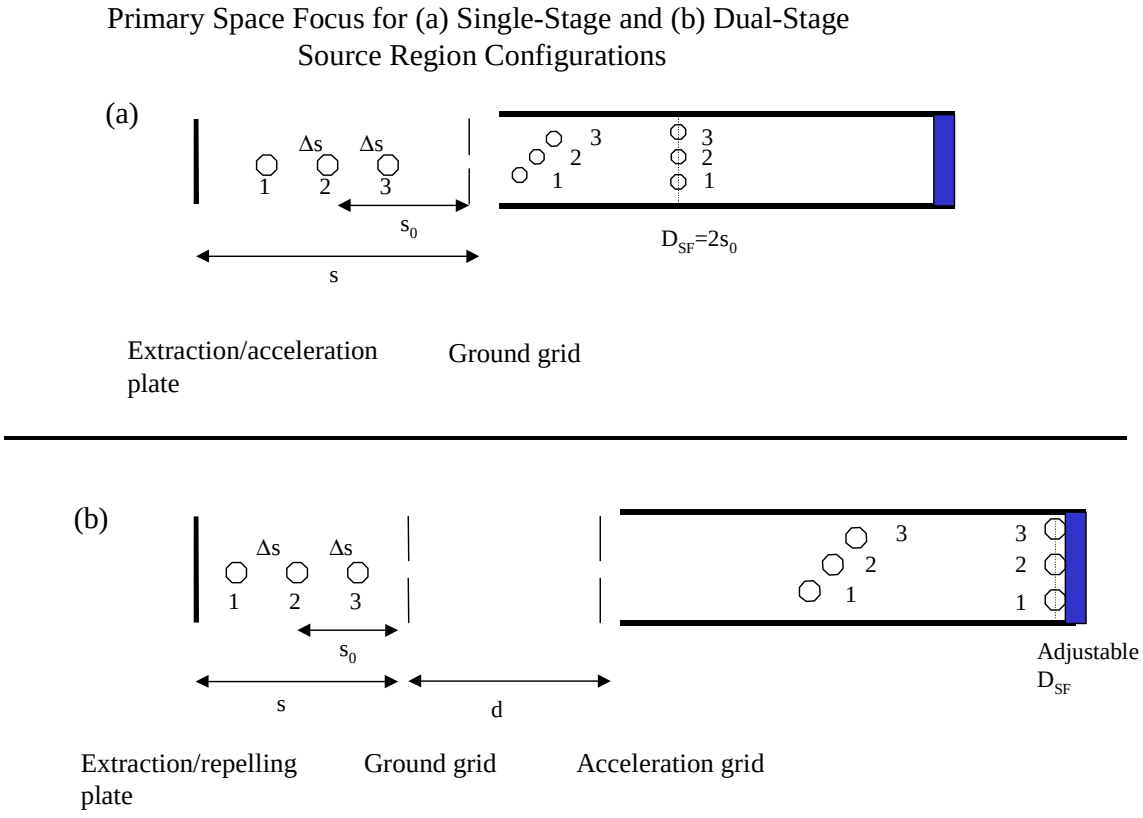

Figure I. 2: Primary space focus principles as illustrated for (a) single-stage extraction/acceleration and (b) Wiley-McLaren dual-stage extraction and acceleration.

$D_{SF} = 2s_o$. However, this point is so close to the beginning of the flight tube that separation of different masses, which is achieved through a long drift region, is difficult.

A much better solution for space-focusing employs a more complex, dual-stage ionization region of three electrodes, as shown in Figure I.2(b). This design is separated into three distinct regions: (i) the ionization source/extraction region, s, with applied electric field E_s, (ii) the acceleration region, d, with applied electric field E_d, and (iii) the field-free drift region D.

Considering isomass ions again with no initial kinetic energy, an ion formed in the source region is accelerated by both the extraction field (E_s) and acceleration field (E_d) to acquire an energy of

$$U_{TOT} = qsE_s + qdE_d$$

Equation I. 13: Energy of an ion accelerated with a dual-stage configuration.

The total time-of-flight (T) is therefore comprised of the time in the source region (T_s), the time in the acceleration region (T_d), and the time in the drift region (T_D). Expanding each of these individually and substituting the relation between kinetic energy and experimental parameters (equations I.2, I.3, and I.4)[5],

$$T_s = \frac{\sqrt{2m}}{qE_s}(\sqrt{qsE_s})$$

$$T_d = \frac{\sqrt{2m}}{qE_d}(\sqrt{U_{TOT}} - \sqrt{qsE_s})$$

$$T_D = D \times \sqrt{\frac{m}{2qU_{TOT}}}$$

Equation I. 14(a), (b), and (c): Fight time contributions for each stage of a dual-stage ion region instrument.

Assuming the ions have zero initial kinetic energy prior to the extraction pulse and summing each contribution provides the benchmark Wiley-McLaren time-of-flight equation for spatial focusing[5]:

$$T(U,s)_{0,S_0} = \sqrt{\frac{m}{2U_{TOT}}} \times \left(2k_0^{1/2} s_0 + \frac{2k_0^{1/2} d}{k_0^{1/2} + 1} + D \right)$$

where

$$k_0 = \frac{s_0 E_s + dE_d}{s_0 E_s}$$

Equation I. 15: Time-of-flight of an ion through a dual-stage-ion-source TOF-MS.

Equation I.15 shows that the total time-of-flight is dependent on the initial position of ion formation (since U_{TOT} is position-dependent). Differentiating with respect to the initial position ($\partial T/\partial s=0$) yields the space focus, D_{SF}, determined through Equation I.16[5]:

$$D_{SF} = 2s_O k_0^{3/2} \times \left(1 - \frac{1}{k_0 + k_0^{1/2}} \frac{d}{s_0} \right)$$

Equation I. 16: Fundamental Wiley-McLaren space focus equation.

In a linear instrumental geometry, the space focus is adjusted by manipulating the E_d/E_s ratio so that D_{SF} coincides with the placement of the detector. Thus, the initial spatial distribution, but not other resolution-limiting factors, is minimized.

Further expansion to the second derivative ($\partial^2 T/\partial s^2=0$) determines if this time-of-flight is a maximum or minimum, and simplification yields a relation of[5]

$$\frac{d}{s_0} = \frac{k_0 - 3}{k_0}\frac{D}{s_0}$$

Equation I. 17: Second derivative of the time-of-flight with respect to initial ion position.

Wiley and McLaren state that optimal dual-stage space-focusing uses a maximum in the time-of-flight, which is achieved if the right-hand side of Equation I.17 is greater than the left[5].

Some notes about the crucial first-order space-focusing conditions bear mentioning. First, the space focus only minimizes the initial *spatial* distribution in the source region, and the mathematics isolates this issue from other broadening factors. Often, the parameters dictated by the space focus condition contradict resolution optimization for other factors. Secondly, the space focus is mass-independent; minimization of initial spatial distributions of ions of any mass is achieved at this point. The time of arrival at the space focus, of course, will depend on the mass of the ion. Finally, the time-of-flight is a maximum for an ion formed at s_0[34] and less for ions with distributions Δs, so that uncorrected spatial distributions may cause fronting peaks.

I.8.3-- Initial kinetic energy distribution and the reflectron

Perhaps the most detrimental factor to resolution is the broad distribution of initial kinetic energies (and thus velocities) of same-mass ions in the source region. Cotter notes that this is especially problematic for laser-based methods and other desorption techniques[2]. As some examples, the distribution of kinetic energies has been approximated for plasma-induced ablation at 10^3 eV or more[8] and hundreds of electron volts for laser ablation methods[34]. Such effects impart an additional velocity (energy) component that adds to or subtracts from the acceleration and extraction energies. The

[34] C. Su. *Int. J. Mass Spectrom. Ion Processes.* **88** (1989) 21.

true drift energy U_{TOT}, as given by equation I.18, will have the additional initial energy component (U_0) so that

$$U_{TOT} = qsE_s + qdE_d \pm U_0$$

Equation I. 18: Total drift energy considering the initial ion kinetic energy.

The time spent by an ion in each of the three regions of a dual-stage ion source configuration will be affected, but we can assume that the time-of-flight is dominated by travel through the field-free drift tube ($T_D >> T_s + T_d$). The change in the time-of-flight of an ion (ΔT_U) due to the initial kinetic energy variations can be approximated by[12]:

$$\Delta T_U = D \times \sqrt{\frac{m}{2}} \times \left(\frac{1}{\sqrt{qsE_s + qdE_d}} - \frac{1}{\sqrt{qsE_s + qdE_d + U_0}} \right)$$

Equation I. 19: Flight time broadening due to initial kinetic energy distributions.

Referring to this relation, initial energy distributions can be decreased by high extraction and acceleration fields, but this contradicts the primary space focus requirement of a low extraction potential and is of limited effectiveness. Alternatively, U_0 can be decreased through such ion source introduction techniques as supersonic beams[34] and laser desorption followed by jet cooling[35,36].

Instruments incorporating a *Reflectron* most effectively correct the initial kinetic energy spreads of isomass ions in the source region. In a simple conceptual discussion, the correction is based on the principle that the initial kinetic energy of an ion will govern its penetration depth into the reflecting field of this "ion mirror". Ions of higher kinetic energy, due to the additional initial contribution, penetrate farther and thus spend more time in the reflectron. Using the appropriate potentials and geometry, the shorter time

[35] G. Meijer, M.S. de Vries, H. Hunziker, H.R. Wendt. *J. Chem. Phys.* **92** (1990) 7624.

[36] G. Meijer, M.S. de Vries, H. Hunziker, H.R. Wendt. *J. Phys. Chem.* **94** (1990) 4394.

that higher energy ions spend in the flight tubes is nullified by the increased time in the reflecting mirror. The principles are illustrated by the single-stage reflectron as pictured in Figure I.3.

Reflectron Principles-- Initial Kinetic Energy ($\pm U_0$) Correction
(Assuming isomass ions with no spatial distribution in the source/acceleration region)

$$\textbf{True Drift Energy} = U_{TOT} = qE_s s + qE_d d \pm U_o$$

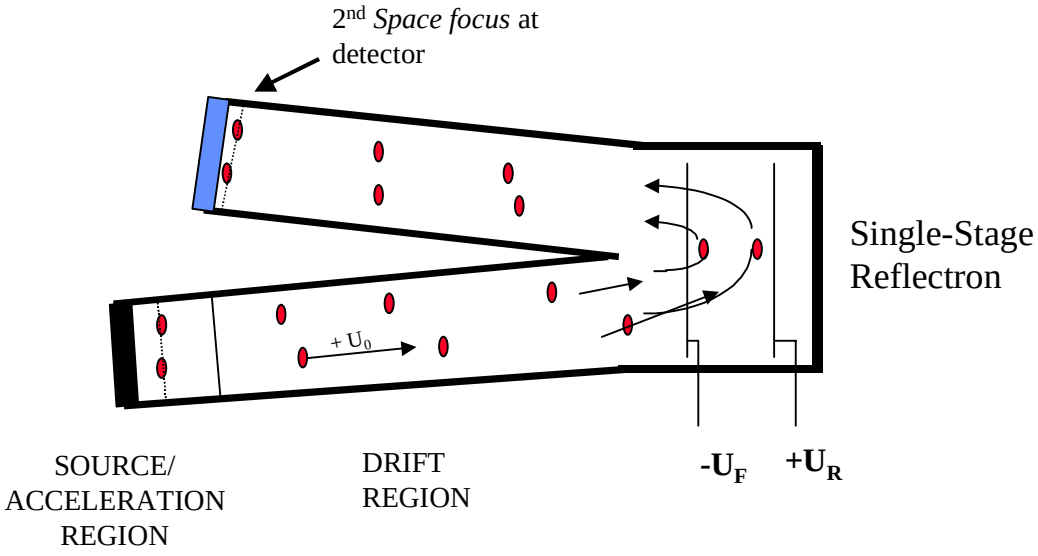

Figure I. 3: Principles of energy-focusing as illustrated in a single-stage reflectron configuration.

The time spent by an ion in a single-stage reflectron (t_{REFL}) can be derived as[2]:

$$t_{REFL} = 2d_{PEN} \times \sqrt{\frac{m}{eU_{TOT}}}$$

Equation I. 20: Time spent by an ion in the reflectron as a function of its penetration depth d_{PEN}.

Eliminating the depth of penetration, d_{PEN}, (an unknown parameter) by relating d_{PEN} to the electric field of the reflectron, E_r, and ion parameters m, U_{TOT}, and q, yields[8]:

$$t_{REFL} = \frac{2d_R}{U_R}\sqrt{\frac{2qU_{TOT}}{m}}$$

Equation I. 21: Time spent by an ion in the reflectron as a function of reflectron parameters.

where d_R is the distance between the electrodes and U_R is the potential field difference between the electrodes.

With these single-stage principles understood, a dual-stage reflectron for second-order focusing, such as our instrument employs, can be discussed. Referring to Figure I.4, the only difference in design is the third electrode, the negative grid. By placing the primary space focus near the beginning of the reflectron, the space-focal plane can act as a "pseudo ion source"[32]. Isomass ions at this plane will have corrected initial spatial-distributions, but uncorrected initial kinetic energy distributions[33,37]. Inside the reflectron, the point where ions are stopped and turned around (dependent on the initial kinetic energy) can mimic the ion source of a linear instrument; however, the different penetration/flight lengths will have minimized initial kinetic energy distributions of the ions in the source region. With properly chosen voltages, it is possible to create a second

[37] U. Boesl, R. Weinkauf, C. Weikhardt, E. Schlag. *Int. J. Mass Spectrom. Ion Processes.* **131** (1994) 87.

Dual-Stage Reflectron schematic (for positive ion reflection)

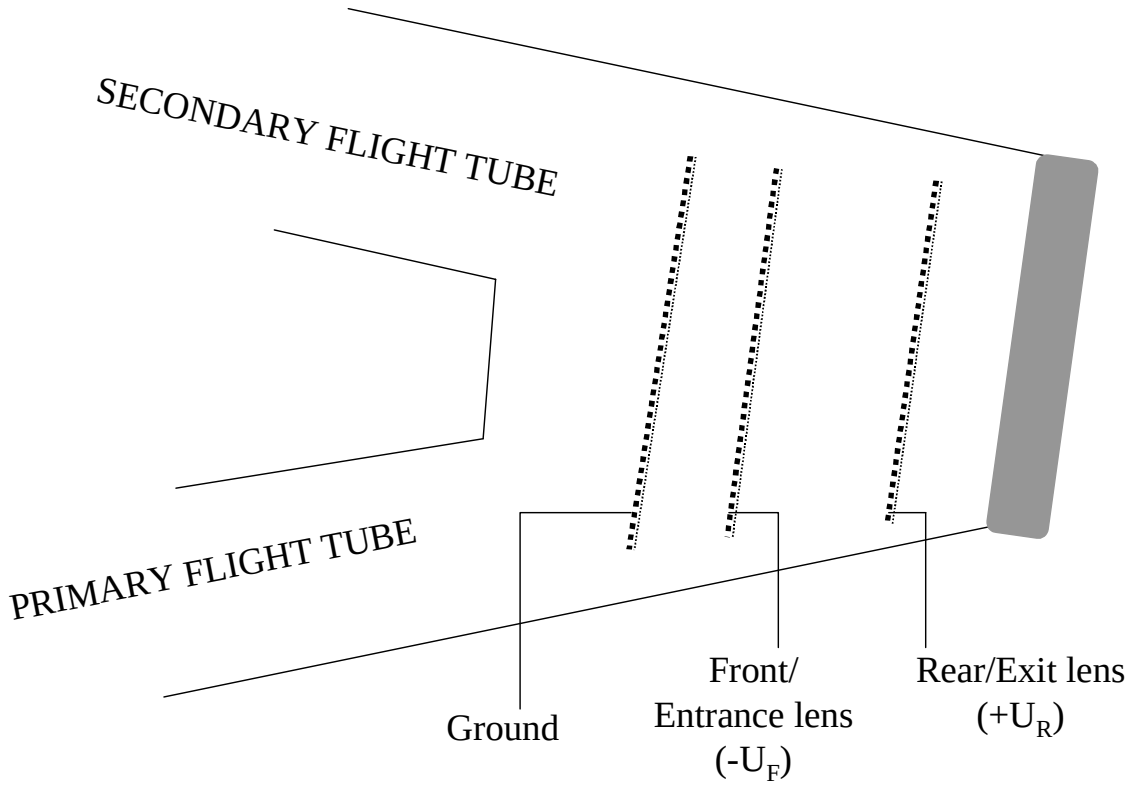

Figure I. 4: Dual-stage reflectron.

order, *secondary space focus* at the end of the final flight tube onto the detector surface. The reflectron thus minimizes peak broadening due to same-mass ions possessing different initial energies at the time of ion extraction.

The reflectron has numerous benefits in the TOF-MS. Primarily, the increased resolution through energy focusing has spurned a resurgence in TOF-MS. As resolution improvements of over an order of magnitude are typical, laser ion sources and reflectron instruments match perfectly[8,33]. Furthermore, sharper peak shapes result from fewer ions in the "tails" of the peaks, as they will have substantially different times-of-flight from the major ion packet and be "smeared out" in the baseline[8]. Also, an increased flight time

from the longer drift length can be achieved without substantially decreasing the acceleration potential and causing detection inefficiencies. Not only is separation of different masses improved without significantly widening each isomass peak, but also turn-around-times and space-charge effects are proportionately decreased in the longer time-of-flight. Finally, and perhaps most importantly for practical instrument operation, the parameters E_s and E_d of the ion source can be experimentally optimized to minimize whatever particular broadening factors harm the analysis without strictly adhering to the primary space focusing conditions.

Other novel applications and modifications of the reflectron illustrate its usefulness. Multiple reflections have been employed[34,38] for improved resolution. In addition, concurrent monitoring of low-energy reflected ions and high-energy ions that penetrate through the reflectron is possible by placing a detector behind the reflecting grids[12]. To reduce the slight angle-dependent peak broadening of the typical angled reflectron, unique "linear reflectrons" have been constructed to decrease ion beam divergence[39].

The reflectron also allows secondary mass spectra to be obtained of any selected parent ion[37]. Secondary laser photoionization is accomplished at the primary space focus at the time that a selected ion packet passes this point. The reflectron then separates the daughter ions that are produced, and tandem MS is accomplished in a single instrument.

I.8.4-- Metastable decay

Metastable decay of a parent molecule into two or more fragments, common with organic TOF-MS samples, poses another resolution problem. Short decay times (in the low microsecond range[37]), where fragmentation occurs in the ionization or acceleration region, can be distinguished due to the position-dependent acceleration energy which an ion receives. Such effects often limit resolution in linear mode instruments as the fragmentation causes slight changes in the time-of-flight. On the other hand, information on decay rates can be ascertained if the parent and fragment peaks can be resolved.

[38] T. Cornish, R. Cotter. Chap. 6, in R. Cotter, Ed. *Time-of-Flight Mass Spectrometry*. Proceedings of the 204th National Meeting of the ACS and Pittsburgh Conference on Analytical Instrumentation. American Chemical Society, Washington, D.C., 1994.

[39] B.A. Mamyrin, V.I. Karataev, D.V. Shmitts, Russian Patent, No. 516306.

Again considering only a simple linear system, if decay occurs in the field-free drift region it is undetectable, since the velocities of both the parent and the fragment are identical. Both species have already experienced the same acceleration in the ion source region and remain at the original velocity of the unfragmented parent. Of course, the various fragments will now possess different kinetic energies due to their identical velocities but different masses.

The reflectron can be used for metastable-decay studies. Even decay in the field-free region can be detected as the smaller daughter fragments, although all possessing the same velocity, will have different, mass-dependent kinetic energies. The kinetic energy of each fragment can be calculated from Equation I.22:

$$U_F = U_A \times \frac{m_F}{m_A}$$

Equation I. 22: Kinetic energy of a metastable fragment species from the parent ion.
where U_F and m_F are the kinetic energy and mass of the fragment, and U_A and m_A are the kinetic energy and mass of the parent ion, respectively.

The differences in kinetic energy can be distinguished by manipulating the reflectron potentials to separate the various fragments and the parent peak[40].

I.8.5-- Temporal distributions

The simplest category of resolution-deterring factors, the pure temporal distribution (σ_{t0}), adds a constant time, t_0, to the total time-of-flight of an ion. Considering again only ions of a single mass, it arises when some ions are formed and thus accelerated at slightly different times from the majority of the ions in the packet. Reducing the ionization laser pulse length and decreasing the rise time of the extraction voltage source can instrumentally minimize the finite time of ion formation and extraction. Also, its effect can be minimized proportionally through longer times-of-flight.

[40] U. Boesl. H. Neuser. R. Weinkauf, E. Schlag. *J. Phys. Chem.* **86** (1982) 4857.

I.8.6-- "Turn-around-time" peak broadening

Somewhat related to both the energy/velocity and spatial distributions, "turn-around-time" ($t_{\pm}$) effects broaden the ion packet. With a gaseous sample, thermal energies of the molecules result in motion along the flight tube axis in a direction away from the drift region. A similar problem often accompanies laser desorption/ablation techniques as ions are ejected from the sample surface with velocities in a variety of directions. Considering an ion at the flight tube axis that is travelling away from the flight tube direction, it must first decelerate and then re-accelerate back to its original location. Therefore, the additional "turn-around-time" contributes to the peak width. In terms of system parameters and the ion's initial velocity (energy) along the flight tube axis[32],

$$t_{\pm} = 2 \times \frac{\sqrt{2mU_{0x}}}{qE_s}$$

Equation I. 23: Turn-around-time of an ion moving in the source region in away from the flight tube.

where q is the charge of the ion and has replaced ze, E_s is the extraction/acceleration potential field, and U_{ox} is the ion's initial energy along the flight tube axis.

To decrease turn-around-time peak broadening, the initial velocity distributions of the ions can be decreased. Alternatively, using a higher extraction voltage (increased E_s) minimizes the time required for the ion to stop and be redirected forward back to the original point of ion formation. In addition, the extraction/acceleration plate can be pulsed with a minimal delay after the ionization laser pulse[33]. Similar to the pure temporal distribution, the turn-around-time cannot be corrected by energy- or space-focusing.

I.8.7-- Space-charge effects

Space-charge broadening, caused by the Coulombic repulsion of like-charge ions, is especially pronounced with the high ion densities in the source region produced by laser desorption/ablation[33]. These like-like repulsions accelerate ions away from the

center of the ion packet to increase the energetic distributions, spatial spreads, and turn-around-time contributions to broaden the peak width. Because such collisions are mass dependent, a variety of ions in the source region will be affected differently; a smaller-mass ion will be more affected in a collision with a larger-mass ion. With a limited area of entrance through the grids into the flight tube, decreases in transmission and signal intensity often accompany the loss in resolving power[33].

Decreasing the number of ions in the source region is an obvious correction for space-charge effects, but this concurrently decreases the sensitivity of the measurement. Reducing the time between ionization and ion extraction, or increasing the extraction voltage may help minimize space-charge broadening.

I.8.8-- Minor peak-broadening factors

Other seemingly minor factors can accumulate to reduce resolution. Instabilities in the electronic recording device and jitter in the triggering/time synchronization of ion extraction events have traditionally been problematic. Further instrumental effects such as electric field fluctuations and fringe electric fields around the voltage plates, lenses, and grids reduce the sharpness of the ion packet. In addition, solid samples with high surface irregularities may result in different flight lengths for species produced from different locations of the sample[32]. Also with solid samples, repeated laser ablation of the same spot forms ions from different depths in the ablated crater leading to slight time-of-flight variations.